Null energy condition violation during inflation and pulsar timing array observations

Gen Ye,[a,b] **Mian Zhu**[c,*] **and Yong Cai**[a,*]

[a]*School of Physics and Microelectronics, Zhengzhou University,*
Zhengzhou, Henan 450001, China

[b]*Institute Lorentz, Leiden University,*
P.O. Box 9506, Leiden 2300 RA, The Netherlands

[c]*Faculty of Physics, Astronomy and Applied Computer Science, Jagiellonian University,*
30-348 Krakow, Poland

E-mail: ye@lorentz.leidenuniv.nl, mian.zhu@uj.edu.pl, caiyong@zzu.edu.cn

ABSTRACT: Recently, evidence of stochastic gravitational wave background (SGWB) signals observed by pulsar timing array (PTA) collaborations, has prompted investigations into their origins. We explore the compatibility of a proposed inflationary scenario, incorporating an intermediate null energy condition (NEC)-violating phase, with the PTA observations. The NEC violation potentially amplifies the primordial tensor power spectrum, offering a promising explanation for PTA observations. Numerical analyses, primarily focused on NANOGrav's 15-year results, reveal the model's compatibility with PTA data. Notably, the model predicts a nearly scale-invariant GW spectrum in the mHz frequency range, which sets our scenario apart from other interpretations predicting a red primordial GW spectrum on smaller scales.

---

*Corresponding author.

Contents

1 Introduction

Gravitational Waves (GWs) are promising tools for exploring the physics of the early universe. Observations of GWs from binary pulsar systems [1] and the merger of binary black holes [2] have ushered in the era of GW detection. Recently, pulsar timing array (PTA) collaborations, including NANOGrav [3, 4], EPTA [5], PPTA [6], and CPTA [7], announced compelling evidence of a signal consistent with stochastic gravitational wave background (SGWB) at the reference frequency $f = 1\,\mathrm{yr}^{-1}$. Shortly after the release of the PTA results, various studies emerged regarding the possible origin of the observed signal, see, e.g., [8–75].

Primordial GWs [76–78], which are the tensor fluctuations generated quantum mechanically in the very early universe, serve as an important possible source of the SGWB. Detecting the primordial GW background would provide valuable physical insights into the origin and evolution of the universe. It is intriguing to explore whether recent observations by PTA can be interpreted as signals of the primordial GWs with a blue-tilted power spectrum. Recently, a lot of research has been conducted in this direction, see, e.g., [21, 55, 56, 61, 79–82].

Inflation [83–86], as a leading paradigm for the very early universe, elegantly addresses the horizon and flatness problems of the Big Bang cosmology. It also predicts a nearly scale-invariant power spectrum of scalar perturbations, which is consistent with the cosmic microwave background (CMB) observations. Furthermore, the conventional slow-roll inflationary scenario also predicts a nearly scale-invariant power spectrum of primordial GWs. However, the PTA observations suggest a highly blue tensor spectrum with a spectral index

$n_T = 1.8 \pm 0.3$ [3, 21], which implies the necessity of new physics beyond the scope of conventional slow-roll inflation at certain scales (see e.g. [87–106] for explorations in generating a blue-tilted tensor spectrum within the inflationary scenario).

The violation of the null energy condition (NEC) may play a crucial role in the very early universe (see e.g. [107] for a review). It has been demonstrated that a fully stable NEC violation can be realized in the "beyond Horndeski" theories [108–115], see also [116–121]. Basically, the violation of NEC implies an increase in the Hubble parameter H (i.e., $dH/dt > 0$). Given that the power spectra of scalar and tensor perturbations are proportional to H^2, an intermediate NEC violation during inflation leads to intriguing phenomena of observational interest at certain scales, including: 1) a significant enhancement in the power spectrum of primordial GWs [122, 123], 2) a notable amplification of the parity-violation effect in primordial GWs [124] (see also [125]), 3) the generation of primordial black holes with masses and abundances of observational interest [126], along with the associated scalar-induced GWs. Remarkably, the scenario proposed by [122] naturally yields a broken power-law power spectrum, which may potentially be consistent with observations from both CMB and PTA, see also [55] for recent studies.

In this paper, we examine the predicted primordial GW background from the model proposed by [122] in light of observations from PTA, with a specific focus on the NANOGrav signal. Our paper is organized as follows. In section 2, we provide a brief overview of the background dynamics in our model. Section 3 introduces the power spectrum and its parameterization as predicted by our model. In section 4, we perform numerical comparisons between the primordial GW background predicted by our model and the NANOGrav signal. Section 5 is dedicated to our conclusion.

## 2 Intermediate NEC violation during inflation

2.1 A brief review of the scenario

In our scenario [122], the universe begins with an initial phase of slow-roll inflation characterized by a Hubble parameter $H = H_{\text{inf1}}$. Subsequently, it transitions into a second phase of slow-roll inflation with a significantly larger Hubble parameter, denoted as $H = H_{\text{inf2}}$, after passing through an intermediate stage of NEC violation. During the evolution, the comoving Hubble horizon (i.e., $a^{-1}H^{-1}$) decreases over time, signifying the exit of perturbation modes from the horizon as the universe undergoes accelerated expansion, see figure 1 for an illustration.[1] After crossing the horizon, these perturbation modes remain in the superhorizon regime until they re-enter the horizon during the subsequent radiation-dominated or matter-dominated expansion era.

For the scalar (or tensor) perturbation modes that exit the horizon during the first stage of slow-roll inflation (i.e., $k < k_1$), their power spectrum is nearly scale-invariant, making it consistent with the observations of temperature anisotropy in the CMB. Similarly, the power spectrum of perturbation modes that exit the horizon during the second stage of slow-roll

---

[1]The horizon of scalar perturbations, as defined by $\sqrt{z_s/z_s''}$, can differ from the Hubble horizon, especially during the transition between different phases. Here, we have simplified the analysis by not considering the specific details of this transition.
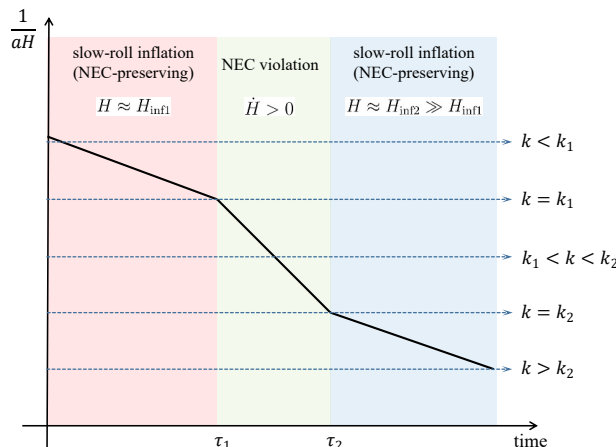
Figure 1. An illustration of the evolution of the conformal Hubble horizon (represented by the solid black lines) and the perturbation modes (depicted as dashed blue lines with arrows) in our scenario.

inflation (i.e., $k > k_2$) is also nearly scale-invariant, but it has a significantly larger amplitude. The scale-invariance of the tensor power spectrum at large scales ensures the absence of a highly suppressed tensor-to-scalar ratio r, and consequently a highly suppressed slow-roll parameter in canonical single-field slow-roll inflation. At small scales, the scale-invariance of the scalar and tensor power spectra prevents them from growing to $\mathcal{O}(1)$, thus preserving the validity of perturbation theory at higher frequencies.

The power spectrum of perturbation modes that exit the horizon during the NEC-violating phase (i.e., $k_1 < k < k_2$) is blue-tilted ($n_s > 0$ or $n_T > 0$). Namely, the violation of the NEC enhances both the scalar and tensor power spectrum by increasing the Hubble parameter H, see [122–124, 126]. Significantly, at the intermediate scales of the scalar power spectrum, the blue tilt and oscillatory features, particularly around the scale corresponding to the beginning of the second inflationary phase, lead to intriguing phenomena of observational interest, including the generation of primordial black holes and the associated scalar-induced GWs [126]. Simultaneously, the power spectrum of tensor perturbations (or the primordial GWs), also exhibits a blue tilt and possesses oscillatory features around the transition scales [122–124]. These distinctive features set our scenario apart from other single-field primordial black hole formation scenarios. The combination of primordial black holes, scalar-induced GW signals, and primordial GWs provides a valuable avenue for studying the violation of the NEC during inflation, especially in the era of multi-messenger and multi-band observations.

Our scenario can be realized with the EFT action (see e.g., [108, 110, 123])

$$S = \int d^4x \sqrt{-g} \left[\frac{M_{\rm P}^2}{2} R - \Lambda(t) - c(t) g^{00} \right. $$
$$\left. + \frac{M_2^4(t)}{2} (\delta g^{00})^2 - \frac{m_3^3(t)}{2} \delta K \delta g^{00} + \frac{\tilde{m}_4^2(t)}{2} R^{(3)} \delta g^{00} \right], \tag{2.1}$$

where $\delta g^{00} = g^{00} + 1$, $R^{(3)}$ is the Ricci scalar on the 3-dimensional spacelike hypersurface, $\delta K = K - 3H$, K is the extrinsic curvature. The time-dependent functions $c(t)$ and $\Lambda(t)$ determine the background evolution, with the relations $c(t) = -M_{\rm P}^2 \dot{H}$ and $\Lambda(t) = M_{\rm P}^2(\dot{H} +$

$3H^2$). The functions $M_2^4(t)$, $m_3^3(t)$ and $\tilde{m}_4^2(t)$ can be determined or constrained based on the condition that the scalar perturbations are in agreement with observations.

Notably, the operator $R^{(3)}\delta g^{00}$ plays a crucial role in preventing scalar perturbations from becoming unstable when the NEC is violated, as demonstrated in [108–110]. The covariant form of action (2.1), as discussed in [111, 112], falls under the category of "beyond Horndeski" theory. Nonetheless, the propagation of primordial GWs is exactly the same as that in general relativity at quadratic order. In this paper, we will not delve into the specific formulations of these coefficient functions or the intricacies of the model construction. Instead, we will employ a simplified parameterization of the background evolution for our scenario. Consequently, we can establish a parameterization for the power spectrum of primordial GWs.

2.2 Parametrization of background

We begin with a flat Friedmann-Lemaitre-Robertson-Walker universe described by the metric

$$ds^2 = -dt^2 + a(t)^2 d\vec{x}^2 = a(\tau)^2(-d\tau^2 + d\vec{x}^2)\,, \tag{2.2}$$

where t is the cosmic time and τ is the conformal time, related by $dt = a d\tau$. Throughout this paper, we will use a dot to denote d/dt and a prime to denote $d/d\tau$. We will also define $H \equiv \dot{a}/a$, $\mathcal{H} \equiv a'/a$.

An inflationary stage is commonly characterized by quasi-de Sitter expansion, where the scale factor approximately evolves as $a \propto |\tau|^{-1}$ for $\tau < 0$. Additionally, we will parameterize our NEC-violating stage with a power-law scale factor, i.e., $a(\tau) \propto |\tau|^n$.[2] The full-scale factor can be then parametrized as a piecewise function of τ:

$$a_j(\tau) = a_j(\tau_j)\left(\frac{\tau - \tau_{R,j}}{\tau_j - \tau_{R,j}}\right)^{\frac{1}{\epsilon_j-1}}\,, \quad \tau < \tau_j\,, \tag{2.3}$$

where τ_j is the conformal time at the end of phase j, $j = 1, 2, 3$ corresponds to the first inflation stage, the NEC-violating stage and the second inflation stage, respectively; $\tau_{R,j} = \tau_j - (\epsilon_j - 1)^{-1}\mathcal{H}^{-1}(\tau_j)$ is the integration constant and $\epsilon_j = -\dot{H}/H^2$ is treated as constant during phase j. Since phases 1 and 3 are assumed as slow-roll inflation, we will set $\epsilon_1 \approx \epsilon_3 \approx 0$ for simplicity. As for the NEC-violating phase (i.e., phase 2), we have $\epsilon_2 < 0$, which indicates $-1 < n = (\epsilon_2 - 1)^{-1} < 0$. A specific design of such a model can be found in [122].

The provided parametrization overlooks the details of transitions between different phases, including the specific variations of ϵ near the beginning or the end of the NEC-violating phase. The dynamics of the transition might depend on the specific model. For simplicity, we will describe the transition physics using the matching condition, ensuring the continuity of the scale factor a and its first derivative a' at τ_1 and τ_2. For our purpose, such a simplification will not make a qualitative difference.

Using eq. (2.3) and denoting the beginning and the end time of the NEC-violating stage to be τ_1 and τ_2, respectively, the continuity of a gives

$$a_1(\tau_1) = a_2(\tau_2)\left(\frac{\tau_1 - \tau_{R,2}}{\tau_2 - \tau_{R,2}}\right)^{\frac{1}{\epsilon_2-1}}\,, \quad a_2(\tau_2) = a_3(\tau_3)\left(\frac{\tau_2 - \tau_{R,3}}{\tau_3 - \tau_{R,3}}\right)^{-1}\,. \tag{2.4}$$

---

[2]An exponential parameterization of the scale factor during the NEC-violating stage is employed in appendix A.

The continuity of a' or $\mathcal{H}$ enables us to define the following quantities

$$\bar{\mathcal{H}}_1 \equiv \mathcal{H}(\tau_1)\,, \ \bar{\mathcal{H}}_2 \equiv \mathcal{H}(\tau_2)\,. \tag{2.5}$$

With the help of (2.3), we can solve the integration constants as

$$\tau_{R,1} = \tau_1 + \bar{\mathcal{H}}_1^{-1}\,, \ \tau_{R,2} = \tau_1 - \frac{\bar{\mathcal{H}}_1^{-1}}{\epsilon_2 - 1} = \tau_2 - \frac{\bar{\mathcal{H}}_2^{-1}}{\epsilon_2 - 1}\,, \ \tau_{R,3} = \tau_2 + \bar{\mathcal{H}}_2^{-1}\,. \tag{2.6}$$

Obviously, the consistency of (2.6) requires

$$(\tau_2 - \tau_1)(1 - \epsilon_2) = \bar{\mathcal{H}}_1^{-1} - \bar{\mathcal{H}}_2^{-1} > 0\,. \tag{2.7}$$

In terms of the scale factor and Hubble parameter;

$$\frac{a_2(\tau_2)}{a_2(\tau_1)} = \left(\frac{\bar{\mathcal{H}}_2}{\bar{\mathcal{H}}_1}\right)^{\frac{1}{1-\epsilon_2}}\,, \ \frac{H_2}{H_1} = \left(\frac{\bar{\mathcal{H}}_2}{\bar{\mathcal{H}}_1}\right)^{\frac{\epsilon_2}{\epsilon_2 - 1}}\,, \tag{2.8}$$

where we have defined $H_2 \equiv \bar{\mathcal{H}}_2/a_2(\tau_2)$ and $H_1 \equiv \bar{\mathcal{H}}_1/a_2(\tau_1)$ to be the Hubble parameter at $\tau = \tau_2$ and $\tau = \tau_1$.

3 Primordial gravitational waves

3.1 Tensor perturbations and mode functions

Since the gravity sector is minimally coupled to the matter sector, the quadratic action for tensor perturbation is simply

$$S_T^{(2)} = \int d\tau d^3x \frac{a^2}{8} \left[\gamma_{ij}'^2 - (\partial_k \gamma_{ij})^2\right]\,, \tag{3.1}$$

where we have set the propagation speed of tensor perturbation to be unity (i.e., the speed of light), and $M_{\rm P} = 1$. In the momentum space, the dynamical equation for tensor perturbation is

$$u_k'' + \left(k^2 - \frac{a''}{a}\right) u_k = 0\,, \tag{3.2}$$

where $u_k \equiv \gamma_k^\lambda a/2$ is the mode function and $\lambda = +, \times$ represent two different polarizations.

The parameterization of scale factor, i.e., eq. (2.3), gives

$$\frac{a_j''}{a_j} = \frac{\nu_j^2 - 1/4}{(\tau - \tau_{R,j})^2}\,, \quad \nu_j \equiv \frac{1}{2} + \frac{1}{1 - \epsilon_j}\,. \tag{3.3}$$

Note that $\epsilon_2 < 0$ would result in $1/2 < \nu_2 < 3/2$. As a result, in each phase, the general solution to eq. (3.2) can be expressed in terms of the Hankel function as

$$u_{k,j}(\tau) = \frac{\sqrt{\pi(\tau_{R,j} - \tau)}}{2} \left\{\alpha_j H_{\nu_j}^{(1)}[k(\tau_{R,j} - \tau)] + \beta_j H_{\nu_j}^{(2)}[k(\tau_{R,j} - \tau)]\right\}\,, \tag{3.4}$$

where $H_{\nu_j}^{(1)}$ and $H_{\nu_j}^{(2)}$ are the first and second kind Hankel functions of the ν_j-th order, respectively; α_j and β_j are k-dependent coefficients.

For simplicity, we have assumed $\epsilon_1 \approx \epsilon_3 \approx 0$, which indicates $\nu_1 \approx \nu_3 \approx 3/2$ and the Hankel functions are simply

$$H_{3/2}^{(1)}(x) = \sqrt{\frac{2}{\pi}} \frac{e^{ix}}{x^{3/2}}(-i-x), \quad H_{3/2}^{(2)}(x) = \left[H_{3/2}^{(1)}(x)\right]^*, \tag{3.5}$$

where the asterisk denotes complex conjugation. We impose the Bunch-Davis vacuum initial condition, which gives $|\alpha_1| = 1$ and $\beta_1 = 0$. The other coefficients α_j and β_j for $j = 2, 3$ can be determined with the matching method, which requires the continuities of u_k and u'_k at the transition surface $\tau = \tau_1$ and $\tau = \tau_2$.

More explicitly, we are interested in the final tensor spectrum, which is relevant to $|\alpha_3 - \beta_3|$, namely

$$P_T \equiv \frac{4k^3}{\pi^2} \frac{|u_{k,3}^2|}{a^2} = \frac{2H(\tau_3)^2}{\pi^2}|\alpha_3 - \beta_3|^2. \tag{3.6}$$

We present

$$
\begin{aligned}
\frac{8\sqrt{x_1 y_1}(\alpha_3 - \beta_3)}{\pi(1 - 2\nu_2)} &= H_{\nu_2}^{(1)}(y_2)\left[\left(i - \frac{1}{x_1}\right) H_{\nu_2-1}^{(2)}(x_2) + H_{\nu_2}^{(2)}(x_2)\right]\sin y_1 \\
&+ H_{\nu_2-1}^{(1)}(y_2)\left[\left(i - \frac{1}{x_1}\right) H_{\nu_2-1}^{(2)}(x_2) + H_{\nu_2}^{(2)}(x_2)\right]\left(\cos y_1 - \frac{\sin y_1}{y_1}\right) \\
&- \left[\frac{ix_1 - 1}{x_1} H_{\nu_2-1}^{(1)}(x_2) + H_{\nu_2}^{(1)}(x_2)\right] \\
&\times \left[H_{\nu_2}^{(2)}(y_2)\sin y_1 + H_{\nu_2-1}^{(2)}(y_2)\left(\cos y_1 - \frac{\sin y_1}{y_1}\right)\right],
\end{aligned}
\tag{3.7}
$$

see [123], where we employ

$$x_1 \equiv \frac{k}{\bar{\mathcal{H}}_1}, \quad x_2 = \left(\nu_2 - \frac{1}{2}\right) x_1 \, ; \quad y_1 \equiv \frac{k}{\bar{\mathcal{H}}_2}, \quad y_2 = \left(\nu_2 - \frac{1}{2}\right) y_1, \tag{3.8}$$

and an overall phase factor has been neglected.

3.2 Parametrization of the tensor spectrum

The tensor spectrum provided by (3.7) is complicated, necessitating further simplification. To interpret the PTA data through primordial GWs from our model, the amplitude of primordial GWs must be enhanced from the order of $\mathcal{O}(10^{-11})$, the upper bound on the amplitude of P_T constrained by CMB observations, to 10^{-3} within the PTA range. Given that in our scenario, $n_T < 2$, the NEC violating stage must persist for scales spanning over four orders of magnitude, i.e., $k_2 > 10^4 k_1$. Consequently, we can safely make the approximation $k_2 \ll k_1$.

Next, we observe that the Hankel function behaves as a pure phase factor in the sub-horizon region and as a power-law function in the super-horizon region. This asymptotic behavior allows us to derive approximate expressions for modes exiting the horizon in different stages. For example, for modes exiting the horizon during the second inflation stage, where $k \gg k_2$, leading to $y_1, y_2, x_1, x_2 \gg 1$, each Hankel function can be approximated as a pure phase function, resulting in

$$P_T \simeq P_{T,2} \equiv \frac{2H_2^2}{\pi^2}, \quad k > k_2. \tag{3.9}$$

Similarly, modes exiting the horizon during the first inflation stage satisfy $k < k_1$, for which we have

$$P_T \simeq P_{T,1} \equiv \frac{2H_1^2}{\pi^2}, \quad k < k_1 .\tag{3.10}$$

For perturbation modes that exit the horizon during the NEC-violating stage, the approximate tensor power spectrum is given by

$$P_T \simeq \frac{\Gamma^2(\nu_2)}{\pi}\left(\frac{2\nu_2 - 1}{4}\right)^{1-2\nu_2}\left(\frac{k}{k_2}\right)^{3-2\nu_2}, \quad k_1 < k < k_2 ,\tag{3.11}$$

see [123] for more details. This spectrum shows a blue tilt ($n_T = 3 - 2\nu_2 > 0$) within the range $k_1 < k < k_2$ in our scenario. Since $1/2 < \nu_2 < 3/2$, we have $0 < n_T < 2$. Remarkably, when employing an exponential parameterization for $a_2(\tau)$, we reach $n_T = 2$, as explicitly demonstrated in appendix A.

The above treatment encounters challenges near the transition scales $k \simeq k_1$ and $k \simeq k_2$, where a simple expansion of the Hankel function through its asymptotic behavior is not applicable. However, in the vicinity of the scale $k \simeq k_1$, the corresponding tensor spectrum is expected to be too small for detection in the near future, allowing us to safely overlook the transition feature in this region. Conversely, near the scale $k \simeq k_2$, the tensor spectrum is sufficiently large for potential detection. For $k \gg k_1$, all Hankel functions with arguments x_1, $x_2 \gg 1$ exhibit the asymptotic behavior $H_\nu^{(1)}(x) \propto \exp[i(x - \nu\pi/2 - \pi/4)]$. This characteristic enables us to capture the features of P_T around $k \simeq k_2$ while simplifying the formulation of P_T.

In light of this, we can parametrize P_T as

$$P_T = P_{T,1} + \frac{\pi}{4}(2 - n_T)\frac{k}{k_2}|g(k)|^2 P_{T,2} ,\tag{3.12}$$

where the auxiliary function is defined as

$$g = H_{\frac{3-n_T}{2}}^{(1)}\left[\frac{2-n_T}{2}\frac{k}{k_2}\right]\sin\frac{k}{k_2} + H_{\frac{1-n_T}{2}}^{(1)}\left[\frac{2-n_T}{2}\frac{k}{k_2}\right]\left(\cos\frac{k}{k_2} - \frac{k_2}{k}\sin\frac{k}{k_2}\right) .\tag{3.13}$$

It is important to note that we have replaced ν_2 by the corresponding tensor spectral index $n_T = 3 - 2\nu_2$ in the NEC violating stage. In the limit of $k \ll k_1$, $P_T \approx P_{T,1}$ since the second term in eq. (3.12) becomes negligible compared to $P_{T,1}$. Conversely, for $k \gg k_1$, the second term in eq. (3.12) becomes dominant. Consequently, it ensures that the features around $k \simeq k_2$ are well captured. While this formulation may sacrifice accuracy around the first transition scale $k \simeq k_1$, such a compromise has minimal impact on our interests.

The primordial tensor power spectrum P_T can be converted to the observed GW energy spectrum by [127]

$$\begin{aligned}\Omega_{\mathrm{GW}} &= \frac{k^2}{12a_0^2 H_0^2}\left[\frac{3\Omega_m j_l(k\tau_0)}{k\tau_0}\sqrt{1.0 + 1.36\frac{k}{k_{\mathrm{eq}}} + 2.50\left(\frac{k}{k_{\mathrm{eq}}}\right)^2}\right]^2 P_T \\ &\simeq \frac{1}{24}\left(\frac{k}{H_0}\right)^2\left[\frac{3\Omega_m}{(k\tau_0)^2}\sqrt{1.0 + 1.36\frac{k}{k_{\mathrm{eq}}} + 2.50\left(\frac{k}{k_{\mathrm{eq}}}\right)^2}\right]^2 P_T\end{aligned}\tag{3.14}$$

where $H_0 = 67.8\,\mathrm{km/s/Mpc}$, $\tau_0 = 1.41 \times 10^4\,\mathrm{Mpc}$, $a_0 = 1$, $k_{\mathrm{eq}} = 0.073\,\Omega_m h^2\,\mathrm{Mpc}^{-1}$, Ω_m is the density fraction of matter today, and the wavenumber relates to the frequency as $k = 2\pi f$.

Parameter	Prior
$\log_{10} P_{T,2}$	$[-5, 0]$
n_T	$[0,2]$
$\log_{10} f_c$	$[-9, -5]$

Table 1. Prior choice for spectrum parameters in the MCMC analysis.

4 Numerical results

In this section, we confront the parameterized spectrum (3.12) to the recent PTA data. As explained in the previous section, we are interested in the case $k_1 \ll k \lesssim k_2$ where the tensor spectrum is blue. To this end, the first term in (3.12) is much smaller than the second one, thus we can safely neglect $P_{T,1}$. With this simplification, the theoretical spectrum (3.12) is fully parameterized by three parameters $\{P_{T,2},\ n_T,\ f_c\}$, where we have defined the transition frequency from the NEC-violating stage to the second inflationary stage as $f_c \equiv 2\pi k_2$. We performed Monte Carlo Markov Chain (MCMC) analysis varying $\{P_{T,2},\ n_T,\ f_c\}$ plus the pulsar and nuisance parameters against the most recent public NANOGrav 15yr dataset [4]. Following NANOGrav, we assume two models on the spatial correlation of the signal, uncorrelated common-spectrum red noise (CURN) and Hellings-Down (HD).[3] Theoretically, our model predicts $n_T < 2$. The validity of the perturbation theory requires $P_{T,2} < 1$. See table 1 for our prior choice of the model parameters.

Figure 2 shows the posterior distributions of the tensor spectrum parameters. Data puts lower bounds on $P_{T,2} > 10^{-2}$ (95% C.L.) and $n_T > 1.0$ (95% C.L.). This is to be expected because it is known that the NANOGrav 15yr data includes a $\sim 3\sigma$ detection of GW background near 10^{-8} Hz with $n_T \sim 1.8$. The distribution of f_c is a peak $-8.1 < \log_{10}(f_c/\text{Hz}) < -6.6$, but this should not be confused with a detection. Near f_c, the spectrum transits from $n_T \sim 2$ to $n_T = 0$ with oscillations. Having $f_c > 10^{-8}$ Hz means that data does not favor the shape of transition so it is moved to the right of the data constraining region, see also figure 3. The upper bound on f_c is due to the prior upper bound on $P_{T,2}$. Because data fixes the amplitude of the spectrum near 10^{-8} Hz, f_c and $P_{T,2}$ are strongly positively correlated, as can be seen from the $\log_{10} f_c$ - $\log_{10} P_{T,2}$ contour of figure 2. Therefore, a prior upper bound $P_{T,2} < 1$ gets translated to an upper bound on f_c.

Figure 3 further compares the best-fit theoretical spectrum with violin points measured by NANOGrav. The left panel of figure 3 illustrates the physical energy spectrum of GW denoted as $\Omega_{GW} h^2$. While the NEC-violating phase satisfactorily accounts for the PTA signal, the tensor spectrum originating from the second inflationary phase also falls comfortably within the detection sensitivity of forthcoming space-based GW observatories like LISA [129], Taiji [130], and Tianqin [131]. The right panel of figure 3 zooms into the PTA data-constrained frequency range and plots the PTA timing excess, see [4] for a detailed definition. Only the first few data points detect GW background signal and the theoretical spectrum (solid black

---

[3]CURN assumes spatially uncorrelated signal while HD assumes that the signal at different pulsars has a spatial correlation described by the Hellings-Down curve [128]. The later is the expected spatial correlation of SGWB. See [4] for details.
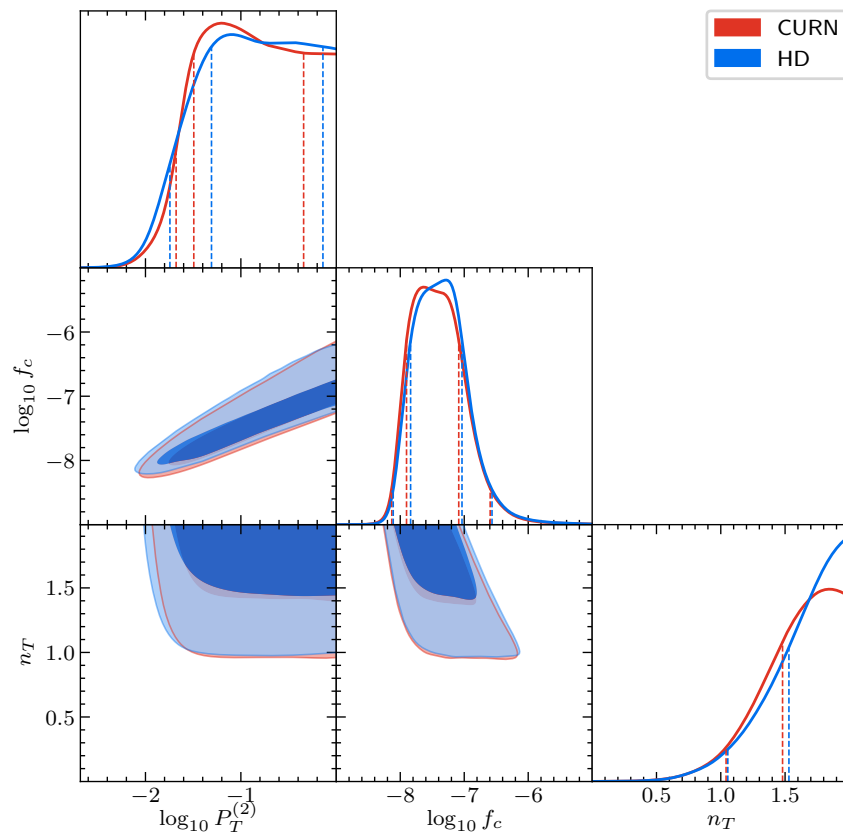
Figure 2. 68% and 95% posterior distributions of model parameters.

(a) $\Omega_{\mathrm{GW}}h^2$

(b) Excess timing
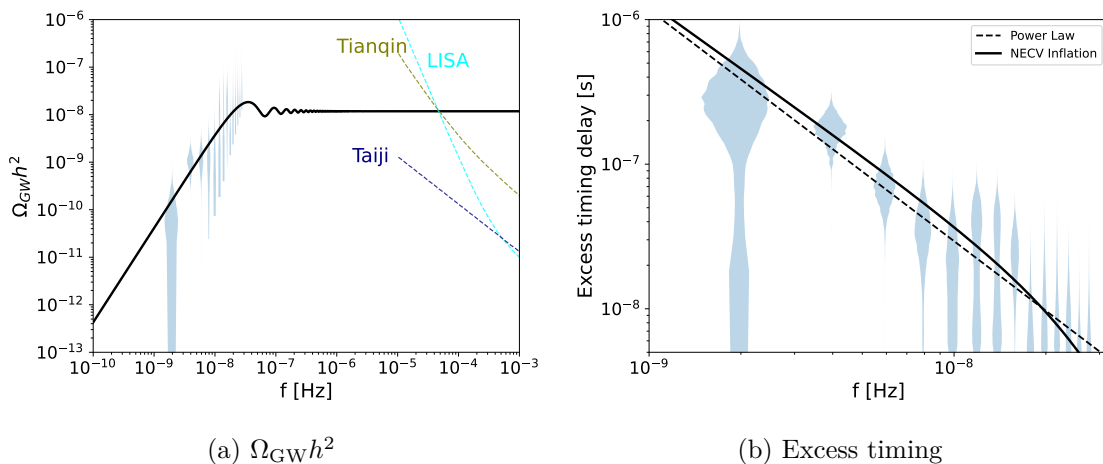
Figure 3. Theoretical spectra with violin data points from NANOGrav 15yr.

line) fits them as well as a power law (dashed black line). Close to f_c, the solid line drops to a smaller n_T, which is not favored by data. Therefore, in the MCMC, f_c automatically shifts to a higher frequency than the range constrained by the data, leading to the observed lower bound on f_c as depicted in figure 2.

The numeric results confirmed that the NEC-violating model can well explain the GW background signal observed by PTA experiments, but the current data is not precise enough to distinguish it from other models, e.g., a simple power law. Our model also predicts a flat tensor spectrum in the mHz frequency range and is detectable to next-generation space GW detectors.

5 Conclusions

The recent SGWB signals reported by PTA collaborations have unveiled a new frontier in the exploration of gravitational wave physics. Notably, if these PTA signals originate from the primordial universe, it necessitates the presence of new physics beyond the standard slow-roll inflation scenario. This necessity arises because PTA observations indicate a highly blue tensor spectrum with a spectral index of $n_T = 1.8 \pm 0.3$, whereas the conventional slow-roll inflation scenario predicts a nearly scale-invariant tensor spectrum.

An intermediate stage of NEC violation during inflation has the potential to amplify the primordial tensor power spectrum on certain scales, offering a potential explanation for the PTA observations. In this paper, we explore the primordial GW spectrum within an inflationary scenario featuring an intermediate NEC-violating phase. We present parameterizations for the background evolution and the GW power spectrum of our model. Our evaluation of the model's compatibility with PTA data reveals its capability to account for the SGWB signal observed by PTA experiments. Given the consistency of signals observed by various PTA experiments, we focus primarily on the NANOGrav 15-year results in the numerical analysis.

Additionally, our model predicts a nearly scale-invariant GW spectrum in the mHz frequency range, potentially detectable by upcoming space-based GW detectors like LISA, Taiji, and Tianqin. This distinctive characteristic distinguishes our scenario from other interpretations predicting a red primordial GW spectrum on smaller scales.

6 Discussions

Intriguingly, ref. [124] found that, for the scenario discussed in this paper, the violation of the NEC naturally amplifies the parity-violating effect as well as its observability in primordial GWs, provided the scalar field determining the background evolution is coupled to a parity-violating term. The wavenumber k corresponding to the maximum of the parity-violating effect is approximately the same as the wavenumber corresponding to the maximum of the power spectrum. This intriguing feature also sets our model apart observationally from other models.

The scale corresponding to the significantly amplified parity-violating effects depends on the scale at which the NEC violation takes place. In this paper, the maximum of the primordial GW power spectrum appears in the vicinity of the PTA band, as shown by the black curve in figure 3. Therefore, the parity violation is still notably amplified in the PTA band. However, considering the power spectrum presented in figure 3, the parity violation is suppressed by the slow-roll condition in the LISA band, as the GW modes in the LISA band are generated during the second slow-roll inflation stage in our scenario. To achieve a notable amplification of the parity-violating effect in the LISA band, it would be necessary for the NEC violation to occur later than what is assumed in the present paper.

In ref. [126], it has been demonstrated that the NEC violation can naturally enhance the primordial scalar power spectrum at certain scales, leading to the production of PBHs and scalar-induced GWs of observational interest. The primordial GWs (i.e., tensor perturbations) primarily depend on the Hubble parameter H. The scalar-induced GWs are induced by scalar perturbations, depending not only on H but also on $\epsilon \equiv -\dot{H}/H^2$ (or its generalized formulation). Therefore, the relative contribution to the GW background of each depends on the specific model's characteristics, particularly the relative magnitudes of the power spectra of scalar and tensor perturbations.

In this paper, we primarily focus on primordial GWs and have not explicitly calculated the primordial scalar perturbations. We assume that the contribution to the GW background in the PTA band mainly comes from primordial GWs rather than scalar-induced GWs. In fact, for the same background evolution, scalar perturbations exhibit stronger model dependence compared to tensor perturbations. In principle, for models constructed with specific covariant action, we can quantitatively compare the contributions of both to the GW background. This remains a subject for future work.

Acknowledgments

A Power spectrum from an exponential parameterization of the scale factor during the NEC-violating phase

In this section, we explicitly calculate the power spectrum P_T using an exponential parameterization for $a_2(\tau)$, representing the scale factor during the NEC-violating stage. This parametrization is frequently used in the study of bouncing cosmology, which also has an NEC-violating phase, see e.g., [136].

The first and second inflationary stages, denoted by $i = 1$ and 3 respectively, are still parameterized by eq. (2.3), with the assumption that $\epsilon_1 \approx \epsilon_3 \approx 0$. Therefore, we have

$$a_1(\tau) = a_1(\tau_1)\frac{\tau_1 - \tau_{R,1}}{\tau - \tau_{R,1}}\,, \ \mathcal{H}_1(\tau) = -\frac{1}{\tau - \tau_{R,1}}\,, \ \tau \le \tau_1 \tag{A.1}$$

and

$$a_3(\tau) = a_3(\tau_3)\frac{\tau_3 - \tau_{R,3}}{\tau - \tau_{R,3}}\,, \ \mathcal{H}_3(\tau) = -\frac{1}{\tau - \tau_{R,3}}\,, \ \tau_2 \le \tau \le \tau_3 \tag{A.2}$$

If the NEC-violating phase is very brief, we can approximate the Hubble parameter as a linear function. As a result, $a_2(\tau)$ can be parameterized by an exponential formulation as

$$a_2(\tau) = a_1(\tau_1)e^{\mathcal{H}_1(\tau_1)(\tau-\tau_1)+\frac{1}{2}\gamma^2(\tau-\tau_1)^2}\,, \ \mathcal{H}_2(\tau) = \mathcal{H}_1(\tau_1) + \gamma^2(\tau - \tau_1)\,, \tag{A.3}$$

where $\tau_1 \le \tau \le \tau_2$.

The parameterization of the background can be related to the characteristic scales:

$$k_1 = \mathcal{H}_1(\tau_1) = (\tau_{R,1} - \tau_1)^{-1} \,, \ \ k_2 = \mathcal{H}_3(\tau_2) = (\tau_{R,3} - \tau_2)^{-1} \,, \tag{A.4}$$

where k_1 is the mode that crosses the horizon at the end of the first inflationary phase, $\tau = \tau_1$, and k_2 is the mode that crosses the horizon at the beginning of the second inflationary phase, $\tau = \tau_2$.

The continuity of a and $\mathcal{H}$ at τ_1 is already incorporated into the parametrization. Therefore, we focus on ensuring continuity at τ_2, which requires that $a_3(\tau_2) = a_2(\tau_2)$ and $\mathcal{H}_3(\tau_2) = \mathcal{H}_2(\tau_2)$, i.e.,

$$\frac{a_3(\tau_2)}{a_1(\tau_1)} = e^{\mathcal{H}_1(\tau_1)(\tau_2-\tau_1)+\frac{1}{2}\gamma^2(\tau_2-\tau_1)^2} \,, \ \ -\frac{1}{\tau_2 - \tau_{R,3}} = \mathcal{H}_1(\tau_1) + \gamma^2(\tau_2 - \tau_1) \,. \tag{A.5}$$

In terms of k_1 and k_2, and considering the condition $k_1 \ll k_2$, we can express

$$k_2 = k_1 + \gamma^2(\tau_2 - \tau_1) \simeq \gamma^2(\tau_2 - \tau_1) \,, \tag{A.6}$$

leading to

$$\tau_2 - \tau_1 \simeq \frac{k_2}{\gamma^2}, \frac{a_3(\tau_2)}{a_1(\tau_1)} \simeq e^{\frac{k_2}{2\gamma^2}(k_2+2k_1)} \simeq e^{\frac{k_2^2}{2\gamma^2}} \,. \tag{A.7}$$

For the first inflationary phase (i.e., $\tau < \tau_1$), the mode function can be given as

$$u_{k,1}(\tau) = \frac{\sqrt{\pi(\tau_{R,1} - \tau)}}{2} H_{3/2}^{(1)}[k(\tau_{R,1} - \tau)] = \frac{e^{ik(\tau_{R,1}-\tau)}}{\sqrt{2}k^{3/2}(\tau_{R,1} - \tau)}[-i - k(\tau_{R,1} - \tau)], \tag{A.8}$$

where we have taken the vacuum initial condition. It can be further simplified to

$$u_{k,1}(\tau) = -\frac{k + ik_1}{\sqrt{2}k^{3/2}} e^{\frac{ik}{k_1}} \,, \ \ \tau < \tau_1 \,. \tag{A.9}$$

In the NEC-violating phase, we have $\epsilon \equiv 1 - \mathcal{H}'/\mathcal{H}^2 \ll -1$, indicating $\mathcal{H}' \gg \mathcal{H}^2$ for nearly the entire phase. As a result, $a''/a = \mathcal{H}^2 + \mathcal{H}' \simeq \mathcal{H}' = \gamma^2$. Consequently, the dynamical equation simplifies to

$$u_{k,2}''(\tau) - \omega_k^2 u_{k,2}(\tau) = 0, \omega_k \equiv \sqrt{\gamma^2 - k^2} \,. \tag{A.10}$$

The parameter ω_k turns imaginary for $k > \gamma$ and real for $k < \gamma$. Yet, we will primarily focus on analyzing the dynamics of perturbations for $k < \gamma$ as it should be adequate for our purposes. In this scenario, ω_k is real, and the general solution takes the form

$$u_{k,2} = c_1 e^{\omega_k \tau} + c_2 e^{-\omega_k \tau} \,. \tag{A.11}$$

The mode function for the second inflationary phase can be expressed as

$$u_{k,3}(\tau) = c_3 \sqrt{\frac{\pi(\tau_{R,3} - \tau)}{2}} J_{\frac{3}{2}}[k(\tau_{R,3} - \tau)] + c_4 \sqrt{\frac{\pi(\tau_{R,3} - \tau)}{2}} Y_{\frac{3}{2}}[k(\tau_{R,3} - \tau)], \tag{A.12}$$

where J and Y are Bessel functions. In a more explicit form, this can be written as

$$u_{k,3}(\tau) = c_3 \left(\frac{\sin z}{z} - \cos z \right) - c_4 \left(\frac{\cos z}{z} + \sin z \right) , \tag{A.13}$$

where $z \equiv k(\tau_{R,3} - \tau)$. On super-horizon scales, the dominating term is c_4, making it sufficient to evaluate c_4. The tensor spectrum on these scales, expressed in terms of c_4, is given by

$$P_T = \frac{4k^3}{\pi^2} \frac{|u_{k,3}^2|}{a^2} = \frac{2H_{\text{inf},2}^2}{\pi^2} 2k|c_4|^2 . \tag{A.14}$$

We match the perturbation at τ_1 and τ_2 for fluctuations with $k < \gamma$, resulting in

$$c_4 = \frac{k^2 + (ik - k_1)(k_1 + \omega_k)}{2\sqrt{2}k^{7/2}\omega_k} e^{\frac{\omega_k}{k_2}} \left[k^2 \sin \frac{k}{k_2} \right.$$
$$\left. + (k_2 - \omega_k) \left(k \cos \frac{k}{k_2} - k_2 \sin \frac{k}{k_2} \right) \right] + (\omega_k \to -\omega_k) . \tag{A.15}$$

A quick check: for modes crossing the horizon in the first inflation phase, we have $k < k_1 \ll k_2$. Moreover, the largeness of $|\epsilon|$ implies $|\epsilon|(\tau_1) = 1 - \frac{\gamma^2}{k_1^2} \gg 1$, or $\gamma \gg k_1 \geq k$, and thus $\omega_k \simeq \gamma$. A series expansion around $k/k_2 \ll 1$ gives

$$c_4 \simeq \frac{(ik - k_1)}{6\sqrt{2}k_2^2 k^{\frac{1}{2}}} e^{\frac{\gamma}{k_2}} (2k_2 + \gamma) + (\gamma \to -\gamma) . \tag{A.16}$$

Therefore, for $k \ll k_1$, the power spectrum is

$$P_{T,\text{inf1}} \simeq \frac{2H_{\text{inf},2}^2}{\pi^2} \times \frac{k_1^2}{k_2^2} \left[\frac{1}{6} e^{\frac{\gamma}{k_2}} \left(2 + \frac{\gamma}{k_2} \right) + (\gamma \to -\gamma) \right]^2$$
$$= \frac{2H_{\text{inf},1}^2}{\pi^2} \frac{a_1^2}{a_2^2} \left[\frac{1}{6} e^{\frac{\gamma}{k_2}} \left(2 + \frac{\gamma}{k_2} \right) + (\gamma \to -\gamma) \right]^2$$
$$\simeq \frac{2H_{\text{inf},1}^2}{\pi^2} \left[\frac{1}{6} \left(2 + \frac{\gamma}{k_2} \right) + \frac{a_1}{a_2} \left(2 - \frac{\gamma}{k_2} \right) \right]^2 \simeq P_{T,\text{inf1}} \left(\frac{1}{3} + \frac{\gamma}{6k_2} \right)^2 , \tag{A.17}$$

which is scale-invariant, as expected. The equation (A.17) indicates that the super-horizon modes generally experience a modification factor during the NEC-violating phase, aligning with results from bouncing cosmology.

Modes with $k > k_2$ and $k > \gamma$ remain sub-horizon at $\tau = \tau_2$ and cross the horizon in the second inflationary phase. Therefore, we can directly write down their corresponding tensor spectrum:

$$P_{T,\text{inf2}} \simeq \frac{2H_{\text{inf},2}^2}{\pi^2} . \tag{A.18}$$

To explain the PTA result, we aim for $P_{T,\text{inf2}} \simeq \mathcal{O}(10^{-4})$. The CMB constraint gives $P_{T,\text{inf1}} \simeq \mathcal{O}(10^{-12})$. Consequently, we can estimate $H_{\text{inf},2}/H_{\text{inf},1} > \mathcal{O}(10^4)$. This estimation provides us with an estimate for γ, i.e.,

$$\frac{H_{\text{inf},2}}{H_{\text{inf},1}} = \frac{\mathcal{H}_2}{\mathcal{H}_1} \frac{a_1}{a_2} > \mathcal{O}(10^4) \; \to \; \frac{k_2}{k_1} e^{\frac{k_2^2}{2\gamma^2}} > \mathcal{O}(10^4) . \tag{A.19}$$
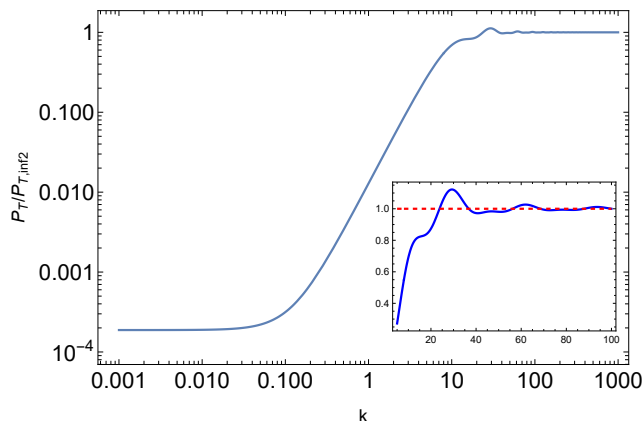
Figure 4. The tensor power spectrum with $k_1 = 0.12$, $k_2 = 10$, $\gamma = 8$.

The exponential function is sensitive to the value of k_2/γ, which suggests that k_2 and γ have the same order of magnitude. For example, if $k_2/\gamma = 10$, it would imply an amplification of the Hubble parameter by e^{50}, an implausible result. Therefore, we could reasonably approximate $P_T = P_{T,\text{inf2}}$ for $k > \gamma$, accepting a minor loss of precision within a narrow scale range.

Obtaining the tensor spectrum for $k > \gamma$ from (A.15) via analytical continuation on ω_k might raise a potential issue. The expression for c_4 displays an apparent discontinuity at $k = \gamma$ and $\omega_k = 0$. Looking into this issue in the limit of $k \to \gamma$, we find

$$\lim_{k \to \gamma} c_4 \simeq \frac{(\gamma^2 - k_2^2) \sin \frac{\gamma}{k_2} + \gamma k_2 \cos \frac{\gamma}{k_2}}{\sqrt{2}\gamma^{\frac{3}{2}}k_2} \; . \tag{A.20}$$

Therefore, c_4 is well-defined at $k = \gamma$. Moreover, for $k \gg \gamma$,

$$c_4 \simeq \frac{1}{2\sqrt{2}k^{\frac{3}{2}}} \left\{ \frac{e^{\frac{i|\omega_k|}{k_2}}}{i|\omega_k|} \left[k^2 \sin \frac{k}{k_2} - i|\omega_k| \left(k \cos \frac{k}{k_2} - k_2 \sin \frac{k}{k_2} \right) \right] + \text{c.c.} \right\} \; . \tag{A.21}$$

Using $|\omega_k| \simeq k$, it can be further simplified to

$$|c_4| = \frac{1}{\sqrt{2}k^{\frac{1}{2}}} \left| 1 + \mathcal{O}\left(\frac{k_2}{k}\right) \right| \to P_T \simeq \frac{2H_{\text{inf,2}}^2}{\pi^2} = P_{T,\text{inf2}} \; . \tag{A.22}$$

Therefore, we can evaluate P_T with $k > \gamma$ through the analytical continuation of ω_k, which we verified numerically and illustrate in figure 4.

In conclusion, we could adopt the following parametrization for P_T:

$$P_T = \frac{H_{\text{inf,2}}^2}{2\pi^2} |f(k)^2| \, , \tag{A.23}$$

where

$$f(k) = \frac{k^2 + (ik - k_1)(k_1 + \omega_k)}{k^3 \omega_k} e^{\frac{\omega_k}{k_2}} \left[(k_2 - \omega_k) \left(k \cos \frac{k}{k_2} - k_2 \sin \frac{k}{k_2} \right) \right.$$
$$\left. + k^2 \sin \frac{k}{k_2} \right] + (\omega_k \to -\omega_k) \, , \; \omega_k \equiv \sqrt{\gamma^2 - k^2} \; . \tag{A.24}$$

How does this relate to PTA observations? As we can see from figure 4, the tensor spectrum is blue-tilted in the region $k_1 \ll k \ll k_2$. Since γ is comparable to k_2, we also have $\gamma \gg k$ such that $\omega_k \simeq \gamma$. The expression (A.24) simplifies to

$$|f(k)| \simeq \frac{k}{3k_2^2} \left[(2k_2 + \gamma)e^{\frac{\gamma}{k_2}} + (2k_2 - \gamma)e^{-\frac{\gamma}{k_2}} \right] , \qquad (A.25)$$

which predicts a blue spectrum with $n_T = 2$ in the range $k_1 \ll k \ll k_2$. This result is in agreement with that in the main text in the limit $n \to \infty$, as the power-law parametrization $a_2 \propto |\tau|^n$ approaches an exponential function.

However, when $k \sim \gamma$ and $\gamma \neq k_2$, we also observe a blue spectrum from figure 4. Yet, estimating the spectral index analytically becomes challenging in this scenario as we lack a reliable method to estimate ω_k.

Open Access. This article is distributed under the terms of the Creative Commons Attribution License (CC-BY4.0), which permits any use, distribution and reproduction in any medium, provided the original author(s) and source are credited.

References

[1] S.L. Detweiler, *Pulsar timing measurements and the search for gravitational waves*, *Astrophys. J.* **234** (1979) 1100 [InSPIRE].

[2] LIGO SCIENTIFIC and VIRGO collaborations, *Observation of Gravitational Waves from a Binary Black Hole Merger*, *Phys. Rev. Lett.* **116** (2016) 061102 [arXiv:1602.03837] [InSPIRE].

[3] NANOGRAV collaboration, *The NANOGrav 15 yr Data Set: Search for Signals from New Physics*, *Astrophys. J. Lett.* **951** (2023) L11 [arXiv:2306.16219] [InSPIRE].

[4] NANOGRAV collaboration, *The NANOGrav 1 yr Data Set: Evidence for a Gravitational-wave Background*, *Astrophys. J. Lett.* **951** (2023) L8 [arXiv:2306.16213] [InSPIRE].

[5] EPTA and InPTA: collaborations, *The second data release from the European Pulsar Timing Array — III. Search for gravitational wave signals*, *Astron. Astrophys.* **678** (2023) A50 [arXiv:2306.16214] [InSPIRE].

[6] D.J. Reardon et al., *Search for an Isotropic Gravitational-wave Background with the Parkes Pulsar Timing Array*, *Astrophys. J. Lett.* **951** (2023) L6 [arXiv:2306.16215] [InSPIRE].

[7] H. Xu et al., *Searching for the Nano-Hertz Stochastic Gravitational Wave Background with the Chinese Pulsar Timing Array Data Release I*, *Res. Astron. Astrophys.* **23** (2023) 075024 [arXiv:2306.16216] [InSPIRE].

[8] A. Addazi, Y.-F. Cai, A. Marciano and L. Visinelli, *Have pulsar timing array methods detected a cosmological phase transition?*, arXiv:2306.17205 [DOI:10.1103/PhysRevD.109.015028] [InSPIRE].

[9] N. Kitajima and K. Nakayama, *Nanohertz gravitational waves from cosmic strings and dark photon dark matter*, *Phys. Lett. B* **846** (2023) 138213 [arXiv:2306.17390] [InSPIRE].

[10] P. Athron et al., *Can supercooled phase transitions explain the gravitational wave background observed by pulsar timing arrays?*, arXiv:2306.17239 [InSPIRE].

[11] A. Ghoshal and A. Strumia, *Probing the Dark Matter density with gravitational waves from super-massive binary black holes*, arXiv:2306.17158 [InSPIRE].

[12] J. Yang, N. Xie and F.P. Huang, *Implication of nano-Hertz stochastic gravitational wave background on ultralight axion particles*, arXiv:2306.17113 [INSPIRE].

[13] Y. Bai, T.-K. Chen and M. Korwar, *QCD-collapsed domain walls: QCD phase transition and gravitational wave spectroscopy*, *JHEP* **12** (2023) 194 [arXiv:2306.17160] [INSPIRE].

[14] J. Ellis et al., *Gravitational waves from supermassive black hole binaries in light of the NANOGrav 15-year data*, *Phys. Rev. D* **109** (2024) L021302 [arXiv:2306.17021] [INSPIRE].

[15] H.-L. Huang et al., *Supermassive primordial black holes in multiverse: for nano-Hertz gravitational wave and high-redshift JWST galaxies*, arXiv:2306.17577 [INSPIRE].

[16] G. Franciolini, J.A. Iovino, V. Vaskonen and H. Veermae, *Recent Gravitational Wave Observation by Pulsar Timing Arrays and Primordial Black Holes: The Importance of Non-Gaussianities*, *Phys. Rev. Lett.* **131** (2023) 201401 [arXiv:2306.17149] [INSPIRE].

[17] Y.-Y. Li et al., *Primordial magnetic field as a common solution of nanohertz gravitational waves and Hubble tension*, arXiv:2306.17124 [INSPIRE].

[18] N. Kitajima et al., *Gravitational Waves from Domain Wall Collapse, and Application to Nanohertz Signals with QCD-coupled Axions*, arXiv:2306.17146 [INSPIRE].

[19] S. Datta and R. Samanta, *Fingerprints of GeV scale right-handed neutrinos on inflationary gravitational waves and PTA data*, *Phys. Rev. D* **108** (2023) L091706 [arXiv:2307.00646] [INSPIRE].

[20] K. Fujikura, S. Girmohanta, Y. Nakai and M. Suzuki, *NANOGrav signal from a dark conformal phase transition*, *Phys. Lett. B* **846** (2023) 138203 [arXiv:2306.17086] [INSPIRE].

[21] S. Vagnozzi, *Inflationary interpretation of the stochastic gravitational wave background signal detected by pulsar timing array experiments*, *JHEAp* **39** (2023) 81 [arXiv:2306.16912] [INSPIRE].

[22] J. Ellis, M. Lewicki, C. Lin and V. Vaskonen, *Cosmic superstrings revisited in light of NANOGrav 15-year data*, *Phys. Rev. D* **108** (2023) 103511 [arXiv:2306.17147] [INSPIRE].

[23] Z. Wang et al., *The nanohertz stochastic gravitational wave background from cosmic string loops and the abundant high redshift massive galaxies*, *Sci. China Phys. Mech. Astron.* **66** (2023) 120403 [arXiv:2306.17150] [INSPIRE].

[24] S.-Y. Guo et al., *Footprints of Axion-Like Particle in Pulsar Timing Array Data and JWST Observations*, arXiv:2306.17022 [INSPIRE].

[25] C. Han, K.-P. Xie, J.M. Yang and M. Zhang, *Self-interacting dark matter implied by nano-Hertz gravitational waves*, arXiv:2306.16966 [INSPIRE].

[26] Z.-Q. Shen, G.-W. Yuan, Y.-Y. Wang and Y.-Z. Wang, *Dark Matter Spike surrounding Supermassive Black Holes Binary and the nanohertz Stochastic Gravitational Wave Background*, arXiv:2306.17143 [INSPIRE].

[27] L. Zu et al., *Mirror QCD phase transition as the origin of the nanohertz Stochastic Gravitational-Wave Background*, arXiv:2306.16769 [INSPIRE].

[28] Y.-C. Bi, Y.-M. Wu, Z.-C. Chen and Q.-G. Huang, *Implications for the supermassive black hole binaries from the NANOGrav 15-year data set*, *Sci. China Phys. Mech. Astron.* **66** (2023) 120402 [arXiv:2307.00722] [INSPIRE].

[29] S. Wang, Z.-C. Zhao, J.-P. Li and Q.-H. Zhu, *Implications of Pulsar Timing Array Data for Scalar-Induced Gravitational Waves and Primordial Black Holes: Primordial Non-Gaussianity f_{NL} Considered*, arXiv:2307.00572 [INSPIRE].

[30] T. Broadhurst, C. Chen, T. Liu and K.-F. Zheng, *Binary Supermassive Black Holes Orbiting Dark Matter Solitons: From the Dual AGN in UGC4211 to NanoHertz Gravitational Waves*, `arXiv:2306.17821` [ɪɴSPIRE].

[31] Y.-F. Cai et al., *Limits on scalar-induced gravitational waves from the stochastic background by pulsar timing array observations*, *Sci. Bull.* **68** (2023) 2929 [`arXiv:2306.17822`] [ɪɴSPIRE].

[32] P.F. Depta, K. Schmidt-Hoberg, P. Schwaller and C. Tasillo, *Do pulsar timing arrays observe merging primordial black holes?*, `arXiv:2306.17836` [ɪɴSPIRE].

[33] L. Bian et al., *Gravitational wave sources for Pulsar Timing Arrays*, `arXiv:2307.02376` [ɪɴSPIRE].

[34] G. Franciolini, D. Racco and F. Rompineve, *Footprints of the QCD Crossover on Cosmological Gravitational Waves at Pulsar Timing Arrays*, `arXiv:2306.17136` [ɪɴSPIRE].

[35] X.K. Du, M.X. Huang, F. Wang and Y.K. Zhang, *Did the nHZ Gravitational Waves Signatures Observed By NANOGrav Indicate Multiple Sector SUSY Breaking?*, `arXiv:2307.02938` [ɪɴSPIRE].

[36] Y.-M. Wu, Z.-C. Chen and Q.-G. Huang, *Cosmological Interpretation for the Stochastic Signal in Pulsar Timing Arrays*, `arXiv:2307.03141` [ɪɴSPIRE].

[37] Z. Yi et al., *Scalar induced gravitational waves in light of Pulsar Timing Array data*, *Sci. China Phys. Mech. Astron.* **66** (2023) 120404 [`arXiv:2307.02467`] [ɪɴSPIRE].

[38] Z.-C. Liang et al., *Sensitivity to anisotropic stochastic gravitational-wave background with space-borne networks*, `arXiv:2307.01541` [ɪɴSPIRE].

[39] L.A. Anchordoqui, I. Antoniadis and D. Lust, *Fuzzy Dark Matter, the Dark Dimension, and the Pulsar Timing Array Signal*, `arXiv:2307.01100` [ɪɴSPIRE].

[40] E. Battista, V. De Falco and D. Usseglio, *First post-Newtonian N-body problem in Einstein-Cartan theory with the Weyssenhoff fluid: Lagrangian and first integrals*, *Eur. Phys. J. C* **83** (2023) 112 [`arXiv:2301.08954`] [ɪɴSPIRE].

[41] V. De Falco and E. Battista, *Analytical results for binary dynamics at the first post-Newtonian order in Einstein-Cartan theory with the Weyssenhoff fluid*, *Phys. Rev. D* **108** (2023) 064032 [`arXiv:2309.00319`] [ɪɴSPIRE].

[42] S.-P. Li and K.-P. Xie, *Collider test of nano-Hertz gravitational waves from pulsar timing arrays*, *Phys. Rev. D* **108** (2023) 055018 [`arXiv:2307.01086`] [ɪɴSPIRE].

[43] Y. Xiao, J.M. Yang and Y. Zhang, *Implications of nano-Hertz gravitational waves on electroweak phase transition in the singlet dark matter model*, *Sci. Bull.* **68** (2023) 3158 [`arXiv:2307.01072`] [ɪɴSPIRE].

[44] C. Zhang et al., *Detecting new fundamental fields with pulsar timing arrays*, *Phys. Rev. D* **108** (2023) 104069 [`arXiv:2307.01093`] [ɪɴSPIRE].

[45] L. Liu, Z.-C. Chen and Q.-G. Huang, *Implications for the non-Gaussianity of curvature perturbation from pulsar timing arrays*, `arXiv:2307.01102` [ɪɴSPIRE].

[46] K. Inomata, K. Kohri and T. Terada, *The Detected Stochastic Gravitational Waves and Subsolar-Mass Primordial Black Holes*, `arXiv:2306.17834` [ɪɴSPIRE].

[47] T. Ghosh et al., *Did we hear the sound of the Universe boiling? Analysis using the full fluid velocity profiles and NANOGrav 15-year data*, `arXiv:2307.02259` [ɪɴSPIRE].

[48] X. Niu and M.H. Rahat, *NANOGrav signal from axion inflation*, *Phys. Rev. D* **108** (2023) 115023 [`arXiv:2307.01192`] [ɪɴSPIRE].

[49] R.A. Konoplya and A. Zhidenko, *Asymptotic tails of massive gravitons in light of pulsar timing array observations*, arXiv:2307.01110 [INSPIRE].

[50] P. Di Bari and M.H. Rahat, *The split majoron model confronts the NANOGrav signal*, arXiv:2307.03184 [INSPIRE].

[51] S. Wang, Z.-C. Zhao and Q.-H. Zhu, *Constraints On Scalar-Induced Gravitational Waves Up To Third Order From Joint Analysis of BBN, CMB, And PTA Data*, arXiv:2307.03095 [INSPIRE].

[52] G. Ye and A. Silvestri, *Can the gravitational wave background feel wiggles in spacetime?*, arXiv:2307.05455 [INSPIRE].

[53] S. Balaji, G. Domènech and G. Franciolini, *Scalar-induced gravitational wave interpretation of PTA data: the role of scalar fluctuation propagation speed*, *JCAP* **10** (2023) 041 [arXiv:2307.08552] [INSPIRE].

[54] Z. Zhang et al., *Nano-Hertz gravitational waves from collapsing domain walls associated with freeze-in dark matter in light of pulsar timing array observations*, *Phys. Rev. D* **108** (2023) 095037 [arXiv:2307.11495] [INSPIRE].

[55] J.-Q. Jiang, Y. Cai, G. Ye and Y.-S. Piao, *Broken blue-tilted inflationary gravitational waves: a joint analysis of NANOGrav 15-year and BICEP/Keck 2018 data*, arXiv:2307.15547 [INSPIRE].

[56] M. Zhu, G. Ye and Y. Cai, *Pulsar timing array observations as possible hints for nonsingular cosmology*, *Eur. Phys. J. C* **83** (2023) 816 [arXiv:2307.16211] [INSPIRE].

[57] H. An et al., *Phase transition during inflation and the gravitational wave signal at pulsar timing arrays*, arXiv:2308.00070 [INSPIRE].

[58] D. Hooper, A. Ireland, G. Krnjaic and A. Stebbins, *Supermassive Primordial Black Holes From Inflation*, arXiv:2308.00756 [INSPIRE].

[59] S.F. King et al., *Quantum gravity effects on dark matter and gravitational waves*, *Phys. Rev. D* **109** (2024) 024057 [arXiv:2308.03724] [INSPIRE].

[60] R. Maji and W.-I. Park, *Supersymmetric U(1)$_{B-L}$ flat direction and NANOGrav 15 year data*, *JCAP* **01** (2024) 015 [arXiv:2308.11439] [INSPIRE].

[61] S. Datta, *Explaining PTA Data with Inflationary GWs in a PBH-Dominated Universe*, arXiv:2309.14238 [INSPIRE].

[62] S.A. Hosseini Mansoori, F. Felegray, A. Talebian and M. Sami, *PBHs and GWs from $\mathbb{T}^2$-inflation and NANOGrav 15-year data*, *JCAP* **08** (2023) 067 [arXiv:2307.06757] [INSPIRE].

[63] L. Frosina and A. Urbano, *Inflationary interpretation of the nHz gravitational-wave background*, *Phys. Rev. D* **108** (2023) 103544 [arXiv:2308.06915] [INSPIRE].

[64] S. He, L. Li, S. Wang and S.-J. Wang, *Constraints on holographic QCD phase transitions from PTA observations*, arXiv:2308.07257 [INSPIRE].

[65] J. Ellis et al., *What is the source of the PTA GW signal?*, *Phys. Rev. D* **109** (2024) 023522 [arXiv:2308.08546] [INSPIRE].

[66] M. Kawasaki and K. Murai, *Enhancement of gravitational waves at Q-ball decay including non-linear density perturbations*, *JCAP* **01** (2024) 050 [arXiv:2308.13134] [INSPIRE].

[67] S. Kawai and J. Kim, *Probing the inflationary moduli space with gravitational waves*, *Phys. Rev. D* **108** (2023) 103537 [arXiv:2308.13272] [INSPIRE].

[68] G. Bhattacharya et al., *Evading no-go for PBH formation and production of SIGWs using Multiple Sharp Transitions in EFT of single field inflation*, `arXiv:2309.00973` [ɪɴSPIRE].

[69] M.X. Huang, F. Wang and Y.K. Zhang, *The Interplay Between the Muon $g-2$ Anomaly and the PTA nHZ Gravitational Waves from Domain Walls in NMSSM*, `arXiv:2309.06378` [ɪɴSPIRE].

[70] K.D. Lozanov et al., *Axion Universal Gravitational Wave Interpretation of Pulsar Timing Array Data*, `arXiv:2310.03594` [ɪɴSPIRE].

[71] R.C. Bernardo and K.-W. Ng, *Beyond the Hellings-Downs curve: Non-Einsteinian gravitational waves in pulsar timing array correlations*, `arXiv:2310.07537` [ɪɴSPIRE].

[72] Z.-C. Chen, S.-L. Li, P. Wu and H. Yu, *NANOGrav hints for first-order confinement-deconfinement phase transition in different QCD-matter scenarios*, `arXiv:2312.01824` [ɪɴSPIRE].

[73] M. Ahmadvand, L. Bian and S. Shakeri, *Heavy QCD axion model in light of pulsar timing arrays*, *Phys. Rev. D* **108** (2023) 115020 [`arXiv:2307.12385`] [ɪɴSPIRE].

[74] D. Chowdhury, A. Hait, S. Mohanty and S. Prakash, *Ultralight $(L_\mu - L_\tau)$ vector dark matter interpretation of NANOGrav observations*, `arXiv:2311.10148` [ɪɴSPIRE].

[75] M. Aghaie, G. Armando, A. Dondarini and P. Panci, *Bounds on Ultralight Dark Matter from NANOGrav*, `arXiv:2308.04590` [ɪɴSPIRE].

[76] L.P. Grishchuk, *Amplification of gravitational waves in an istropic universe*, *Zh. Eksp. Teor. Fiz.* **67** (1974) 825 [ɪɴSPIRE].

[77] A.A. Starobinsky, *Spectrum of relict gravitational radiation and the early state of the universe*, *JETP Lett.* **30** (1979) 682 [ɪɴSPIRE].

[78] V.A. Rubakov, M.V. Sazhin and A.V. Veryaskin, *Graviton Creation in the Inflationary Universe and the Grand Unification Scale*, *Phys. Lett. B* **115** (1982) 189 [ɪɴSPIRE].

[79] D. Borah, S. Jyoti Das and R. Samanta, *Inflationary origin of gravitational waves with Miracle-less WIMP dark matter in the light of recent PTA results*, `arXiv:2307.00537` [ɪɴSPIRE].

[80] S. Choudhury, *Single field inflation in the light of NANOGrav 15-year Data: Quintessential interpretation of blue tilted tensor spectrum through Non-Bunch Davies initial condition*, `arXiv:2307.03249` [ɪɴSPIRE].

[81] I. Ben-Dayan, U. Kumar, U. Thattarampilly and A. Verma, *Probing the early Universe cosmology with NANOGrav: Possibilities and limitations*, *Phys. Rev. D* **108** (2023) 103507 [`arXiv:2307.15123`] [ɪɴSPIRE].

[82] V.K. Oikonomou, *Flat energy spectrum of primordial gravitational waves versus peaks and the NANOGrav 2023 observation*, *Phys. Rev. D* **108** (2023) 043516 [`arXiv:2306.17351`] [ɪɴSPIRE].

[83] A.H. Guth, *The Inflationary Universe: A Possible Solution to the Horizon and Flatness Problems*, *Phys. Rev. D* **23** (1981) 347 [ɪɴSPIRE].

[84] A.D. Linde, *A New Inflationary Universe Scenario: A Possible Solution of the Horizon, Flatness, Homogeneity, Isotropy and Primordial Monopole Problems*, *Phys. Lett. B* **108** (1982) 389 [ɪɴSPIRE].

[85] A. Albrecht and P.J. Steinhardt, *Cosmology for Grand Unified Theories with Radiatively Induced Symmetry Breaking*, *Phys. Rev. Lett.* **48** (1982) 1220 [ɪɴSPIRE].

[86] A.A. Starobinsky, *A New Type of Isotropic Cosmological Models Without Singularity*, *Phys. Lett. B* **91** (1980) 99 [inSPIRE].

[87] Y.-S. Piao and Y.-Z. Zhang, *Phantom inflation and primordial perturbation spectrum*, *Phys. Rev. D* **70** (2004) 063513 [astro-ph/0401231] [inSPIRE].

[88] M. Baldi, F. Finelli and S. Matarrese, *Inflation with violation of the null energy condition*, *Phys. Rev. D* **72** (2005) 083504 [astro-ph/0505552] [inSPIRE].

[89] Y.-S. Piao, *Gravitational wave background from phantom superinflation*, *Phys. Rev. D* **73** (2006) 047302 [gr-qc/0601115] [inSPIRE].

[90] T. Kobayashi, M. Yamaguchi and J. Yokoyama, *G-inflation: Inflation driven by the Galileon field*, *Phys. Rev. Lett.* **105** (2010) 231302 [arXiv:1008.0603] [inSPIRE].

[91] T. Kobayashi, M. Yamaguchi and J. Yokoyama, *Generalized G-inflation: Inflation with the most general second-order field equations*, *Prog. Theor. Phys.* **126** (2011) 511 [arXiv:1105.5723] [inSPIRE].

[92] S. Endlich, A. Nicolis and J. Wang, *Solid Inflation*, *JCAP* **10** (2013) 011 [arXiv:1210.0569] [inSPIRE].

[93] Y.-F. Cai et al., *On the possibility of blue tensor spectrum within single field inflation*, *Nucl. Phys. B* **900** (2015) 517 [arXiv:1412.7241] [inSPIRE].

[94] J.-O. Gong, *Blue running of the primordial tensor spectrum*, *JCAP* **07** (2014) 022 [arXiv:1403.5163] [inSPIRE].

[95] D. Cannone, G. Tasinato and D. Wands, *Generalised tensor fluctuations and inflation*, *JCAP* **01** (2015) 029 [arXiv:1409.6568] [inSPIRE].

[96] Y. Wang and W. Xue, *Inflation and Alternatives with Blue Tensor Spectra*, *JCAP* **10** (2014) 075 [arXiv:1403.5817] [inSPIRE].

[97] S. Kuroyanagi, T. Takahashi and S. Yokoyama, *Blue-tilted Tensor Spectrum and Thermal History of the Universe*, *JCAP* **02** (2015) 003 [arXiv:1407.4785] [inSPIRE].

[98] Y. Cai, Y.-T. Wang and Y.-S. Piao, *Is there an effect of a nontrivial c_T during inflation?*, *Phys. Rev. D* **93** (2016) 063005 [arXiv:1510.08716] [inSPIRE].

[99] Y. Cai, Y.-T. Wang and Y.-S. Piao, *Propagating speed of primordial gravitational waves and inflation*, *Phys. Rev. D* **94** (2016) 043002 [arXiv:1602.05431] [inSPIRE].

[100] Y.-T. Wang, Y. Cai, Z.-G. Liu and Y.-S. Piao, *Probing the primordial universe with gravitational waves detectors*, *JCAP* **01** (2017) 010 [arXiv:1612.05088] [inSPIRE].

[101] T. Fujita, S. Kuroyanagi, S. Mizuno and S. Mukohyama, *Blue-tilted Primordial Gravitational Waves from Massive Gravity*, *Phys. Lett. B* **789** (2019) 215 [arXiv:1808.02381] [inSPIRE].

[102] S. Kuroyanagi, T. Takahashi and S. Yokoyama, *Blue-tilted inflationary tensor spectrum and reheating in the light of NANOGrav results*, *JCAP* **01** (2021) 071 [arXiv:2011.03323] [inSPIRE].

[103] S. Akama, S. Hirano and T. Kobayashi, *Primordial tensor non-Gaussianities from general single-field inflation with non-Bunch-Davies initial states*, *Phys. Rev. D* **102** (2020) 023513 [arXiv:2003.10686] [inSPIRE].

[104] S. Akama and H.W.H. Tahara, *Imprints of primordial gravitational waves with non-Bunch-Davies initial states on CMB bispectra*, *Phys. Rev. D* **108** (2023) 103522 [arXiv:2306.17752] [inSPIRE].

[105] W. Giarè, F. Renzi and A. Melchiorri, *Higher-Curvature Corrections and Tensor Modes*, *Phys. Rev. D* **103** (2021) 043515 [arXiv:2012.00527] [inSPIRE].

[106] W. Giarè, M. Forconi, E. Di Valentino and A. Melchiorri, *Towards a reliable calculation of relic radiation from primordial gravitational waves*, *Mon. Not. Roy. Astron. Soc.* **520** (2023) 2 [arXiv:2210.14159] [inSPIRE].

[107] V.A. Rubakov, *The Null Energy Condition and its violation*, *Phys. Usp.* **57** (2014) 128 [arXiv:1401.4024] [inSPIRE].

[108] Y. Cai et al., *The Effective Field Theory of nonsingular cosmology*, *JHEP* **01** (2017) 090 [arXiv:1610.03400] [inSPIRE].

[109] P. Creminelli, D. Pirtskhalava, L. Santoni and E. Trincherini, *Stability of Geodesically Complete Cosmologies*, *JCAP* **11** (2016) 047 [arXiv:1610.04207] [inSPIRE].

[110] Y. Cai, H.-G. Li, T. Qiu and Y.-S. Piao, *The Effective Field Theory of nonsingular cosmology: II*, *Eur. Phys. J. C* **77** (2017) 369 [arXiv:1701.04330] [inSPIRE].

[111] Y. Cai and Y.-S. Piao, *A covariant Lagrangian for stable nonsingular bounce*, *JHEP* **09** (2017) 027 [arXiv:1705.03401] [inSPIRE].

[112] R. Kolevatov, S. Mironov, N. Sukhov and V. Volkova, *Cosmological bounce and Genesis beyond Horndeski*, *JCAP* **08** (2017) 038 [arXiv:1705.06626] [inSPIRE].

[113] A. Ilyas, M. Zhu, Y. Zheng and Y.-F. Cai, *Emergent Universe and Genesis from the DHOST Cosmology*, *JHEP* **01** (2021) 141 [arXiv:2009.10351] [inSPIRE].

[114] A. Ilyas et al., *DHOST Bounce*, *JCAP* **09** (2020) 002 [arXiv:2002.08269] [inSPIRE].

[115] M. Zhu and Y. Zheng, *Improved DHOST Genesis*, *JHEP* **11** (2021) 163 [arXiv:2109.05277] [inSPIRE].

[116] M. Libanov, S. Mironov and V. Rubakov, *Generalized Galileons: instabilities of bouncing and Genesis cosmologies and modified Genesis*, *JCAP* **08** (2016) 037 [arXiv:1605.05992] [inSPIRE].

[117] T. Kobayashi, *Generic instabilities of nonsingular cosmologies in Horndeski theory: A no-go theorem*, *Phys. Rev. D* **94** (2016) 043511 [arXiv:1606.05831] [inSPIRE].

[118] A. Ijjas and P.J. Steinhardt, *Fully stable cosmological solutions with a non-singular classical bounce*, *Phys. Lett. B* **764** (2017) 289 [arXiv:1609.01253] [inSPIRE].

[119] D.A. Dobre et al., *Unbraiding the Bounce: Superluminality around the Corner*, *JCAP* **03** (2018) 020 [arXiv:1712.10272] [inSPIRE].

[120] M. Zhu et al., *Scalar and tensor perturbations in DHOST bounce cosmology*, *JCAP* **11** (2021) 045 [arXiv:2108.01339] [inSPIRE].

[121] Y. Cai, J. Xu, S. Zhao and S. Zhou, *Perturbative unitarity and NEC violation in genesis cosmology*, *JHEP* **10** (2022) 140 [*Erratum ibid.* **11** (2022) 063] [arXiv:2207.11772] [inSPIRE].

[122] Y. Cai and Y.-S. Piao, *Intermittent null energy condition violations during inflation and primordial gravitational waves*, *Phys. Rev. D* **103** (2021) 083521 [arXiv:2012.11304] [inSPIRE].

[123] Y. Cai and Y.-S. Piao, *Generating enhanced primordial GWs during inflation with intermittent violation of NEC and diminishment of GW propagating speed*, *JHEP* **06** (2022) 067 [arXiv:2201.04552] [inSPIRE].

[124] Y. Cai, *Generating enhanced parity-violating gravitational waves during inflation with violation of the null energy condition*, *Phys. Rev. D* **107** (2023) 063512 [arXiv:2212.10893] [inSPIRE].

[125] M. Zhu and Y. Cai, *Parity-violation in bouncing cosmology*, *JHEP* **04** (2023) 095 [arXiv:2301.13502] [INSPIRE].

[126] Y. Cai, M. Zhu and Y.-S. Piao, *Primordial black holes from null energy condition violation during inflation*, arXiv:2305.10933 [INSPIRE].

[127] M.S. Turner, M.J. White and J.E. Lidsey, *Tensor perturbations in inflationary models as a probe of cosmology*, *Phys. Rev. D* **48** (1993) 4613 [astro-ph/9306029] [INSPIRE].

[128] R. Hellings and G. Downs, *Upper limits on the isotropic gravitational radiation background from pulsar timing analysis*, *Astrophys. J. Lett.* **265** (1983) L39 [INSPIRE].

[129] LISA collaboration, *Laser Interferometer Space Antenna*, arXiv:1702.00786 [INSPIRE].

[130] W.-R. Hu and Y.-L. Wu, *The Taiji Program in Space for gravitational wave physics and the nature of gravity*, *Natl. Sci. Rev.* **4** (2017) 685 [INSPIRE].

[131] TIANQIN collaboration, *TianQin: a space-borne gravitational wave detector*, *Class. Quant. Grav.* **33** (2016) 035010 [arXiv:1512.02076] [INSPIRE].

[132] A. Mitridate and D. Wright, *PTArcade*, zenodo (2023).

[133] W.G. Lamb, S.R. Taylor and R. van Haasteren, *Rapid refitting techniques for Bayesian spectral characterization of the gravitational wave background using pulsar timing arrays*, *Phys. Rev. D* **108** (2023) 103019 [arXiv:2303.15442] [INSPIRE].

[134] J.A. Ellis, M. Vallisneri, S.R. Taylor and P.T. Baker, *ENTERPRISE: Enhanced Numerical Toolbox Enabling a Robust PulsaR Inference SuitE*, zenodo (2020).

[135] S.R. Taylor et al., *enterprise_extensions*, https://github.com/nanograv/enterprise_extensions (2021).

[136] Y.-F. Cai, D.A. Easson and R. Brandenberger, *Towards a Nonsingular Bouncing Cosmology*, *JCAP* **08** (2012) 020 [arXiv:1206.2382] [INSPIRE].